Improving MR Image Quality in the Presence of Motion by Using Rephasing Gradients

E. Mark Haacke[1]
Gerald W. Lenz[2]

Numerous techniques exist for suppressing ghosting artifacts due to respiratory motion on MR images. Although such methods can remove coherent ghosting artifacts, motion during gradient pulses also leads to poor image quality. This is due to phase variations at the echo caused by changes in velocity from one phase-encoding view to the next. The effect becomes severe for long sampling times and long TE values and can lead to low estimates of T2. We discuss general, robust modifications of the standard gradient or spin-echo sequences by using rephasing gradients that force the phase of constant-velocity moving spins to be zero at the echo. These sequences lead to a significant reduction in motion artifacts and hence improvement in image quality. They can be applied to multislice, multiecho, water/fat, and gating schemes as well. Since motion problems are universal, it would appear that these modified sequences should come into common usage for MR imaging.

During the past few years, a myriad of techniques have been offered as solutions to the respiratory artifact problem in body imaging. These range from respiratory gating [1], fat suppression using inversion recovery [2] or other techniques [3], pseudogating [4, 5], ordered phase encoding [6, 7], motion modeling [8, 9], and fast imaging [10, 11]. All of these approaches eliminate or reduce artifacts caused by motion between phase-encoding views in the standard two-dimensional Fourier transform (2DFT) spin-echo sequence.

Significant motion in the body, from several millimeters to several centimeters [12], is a universal problem in MR imaging. Motion artifacts may be present in the form of severe ghosting or as a subtle loss of signal due to spin dephasing across a pixel. Evidently, a major source of ghosting and loss of signal in everyday imaging is due to imperfect refocusing of the moving spins at the echo. We propose the use of extra pulses to rephase constant-velocity moving spins. The success of the new rephasing sequence is not dependent on the value that the velocity assumes. Furthermore, these gradients can be applied to all three spatial directions to ensure optimal refocusing regardless of the direction of the motion. The blurring that occurs due to the motion itself still needs to be corrected by one of the techniques mentioned earlier, but generally blurring is not the major problem.

Theory

The standard 2DFT spin-echo method refocuses stationary spins so that their phase is zero at the echo. For constant-velocity moving spins, the phase is not zero at the echo, [13, 14] and this is best illustrated by evaluating the phase behavior for the sequence in Figure 1A. The sampling time t is defined to be zero at the echo. Only constant-velocity spins are considered, so that the time depen-

Received December 1, 1986; accepted after revision February 2, 1987.

[1] Departments of Radiology and Physics, Case Western Reserve University and University Hospitals of Cleveland, 2074 Abington Rd., Cleveland, OH 44106. Address reprint requests to E. M. Haacke at University Hospitals of Cleveland.

[2] Departments of Radiology and Electrical Engineering and Applied Physics, Case Western Reserve University and University Hospitals of Cleveland, Cleveland, OH 44106.

AJR 148:1251–1258, June 1987
0361–803X/87/1486–1251

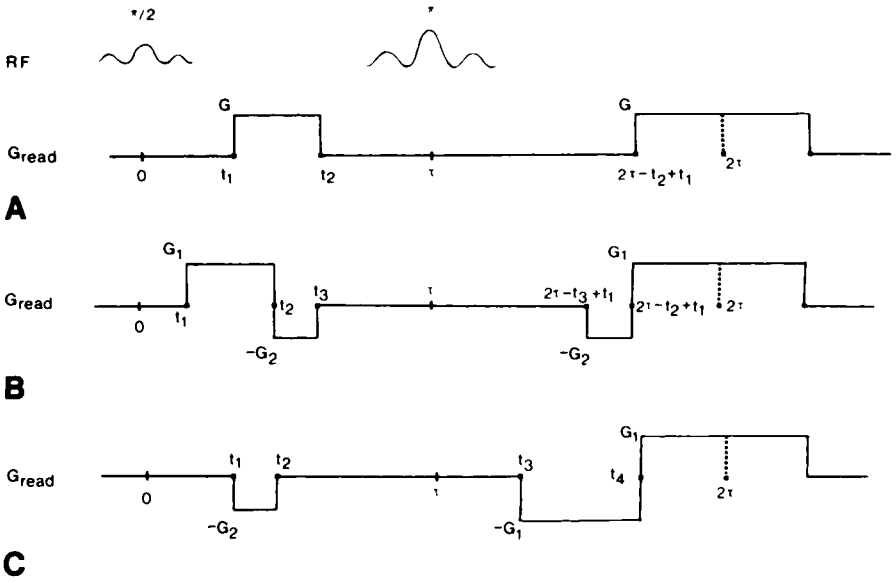

Fig. 1.—*A*, Example of standard spin-echo sequence for applied RF and read gradient fields. Echo time (TE) is 2τ. Dephasing portion of read gradient is before the π-pulse to allow for short echo times. G = gradient; t = time.

***B*, A modified spin-echo sequence with rephasing gradients to ensure zero phase at the echo for constant-velocity and stationary spins. The sequence can be designed so that the phase is zero at the echo for all velocities or so that incomplete refocusing occurs and yet enough signal remains so that sufficient phase information persists to estimate velocity. Timings reflect symmetry inherent in this bipolar design.**

***C*, A rephased spin-echo sequence similar to that in *B*, but with first pair of bipolar gradients replaced by a single dephasing gradient. Timings here are left general and are determined by optimizing the sequence for a given TE value.**

dence of a spin starting at a position x is

$$x(t') = x + vt' \tag{1}$$

at time t' later. The phase at any time $t + 2\tau$ (i.e., during sampling) for a spin starting at position x at the center of the $\pi/2$ pulse is

$$\phi(x, t) = -\gamma G \int_{t_1}^{t_2} x(t')\,dt' + \gamma G \int_{2\tau - t_2 + t_1}^{2\tau + t} x(t')\,dt' \tag{2}$$

$$= \gamma G x t + \gamma G v[(t_2 - t_1)(2\tau - t_2) + 2\tau t + \tfrac{1}{2}t^2] \tag{3}$$

where v = velocity, G = gradient, γ = gyromagnetic ratio. The first term, γGxt, is the expected phase behavior for stationary spins, while the last three terms are due to the constant-velocity motion. The second is the constant-phase-shift term at the echo (where $t = 0$)

$$\phi(x, 0) = \gamma G v(t_2 - t_1)(2\tau - t_2) \tag{4}$$

The third term, $2\gamma Gv\tau t$, is an extra linear phase shift and leads to the spins appearing in the image at the point x', where

$$x' = x + 2\tau v \tag{5}$$

The fourth term, $\frac{1}{2}\gamma Gvt^2$, is quadratic in time and leads to a loss of resolution in the image since it acts as a complex filter [14]. All of the last three terms can lead to ghosting if v changes from view to veiw.

The amplitude of these last three terms will determine the role each plays in affecting the image. For example, for τ = 30 msec (or TE = 60 msec), G = 1 mT/m, a 30-cm field of view, a sampling interval of 80 μsec, 256 sampling points, t_1 = 10 msec and t_2 = 20 msec, the phase shift at the echo (from equation 4) is $1.07v$ radians where v is in cm/sec. The position shift is $0.06v$ in cm, and the phase error at the end of sampling from the term quadratic in time is $0.013v$ radians. The first two terms are thus seen to be the most significant.

This phase behavior of the signal for moving spins suggests that respiratory motion alone may not be the major source of ghosting in body imaging. Yet respiratory motion along the phase-encoding direction of just Δy = 0.2 cm between views has been shown [7] to give significant ghosting. It is instructive to examine the change in phase, $\Delta\phi$, of a spin from one phase-encoding view to the next:

$$\Delta\phi_m = \gamma \Delta G_y t_y \Delta y \tag{6a}$$

$$= \gamma G \Delta t \Delta y \tag{6b}$$

when the fields of view in both x and y are equal. Here ΔG_y is the increment of the phase-encoding gradient and t_y its duration. Similarly, for motion a distance Δx along the read direction, the maximum phase change across a sampling interval, Δt, is

$$\Delta\phi_m = \gamma G \Delta t \Delta x \tag{7}$$

Both these phase changes represent only 0.04 radians when $\Delta x = \Delta y$ = 0.2 cm. We also know that as the amplitude of the motion increases, so does the amplitude of the ghosting [7]. With respiratory amplitudes of 0.5 cm, the phase change is 0.1 radians and the ghosts can be as large as 10% of the original image amplitude.

In order to appreciate the importance of the phase terms in equation 4, it is useful to find out what velocities lead to the same phase variations as motion between views. The worst possible spin-echo sequence occurs when the RF pulses are assumed to be instantaneous and the sampling time is taken to be 2τ. The phase change from view to view is then

$$\Delta\phi_v = \tfrac{1}{4}\,\gamma G v (\mathrm{TE})^2 \tag{8}$$

Equating expressions 6b or 7 with 8 and setting $\Delta a = \Delta x = \Delta y$ gives the condition

$$v_e = \frac{4\Delta a \Delta t}{(\mathrm{TE})^2} \tag{9}$$

for the velocity change from view to view where motion during gradient pulses causes the same ghosting as the usual motion between views. However, in the more realistic example above using $\tau = 30$ msec in equation 4 gives roughly

$$v_e = \frac{9\Delta a \Delta t}{(TE)^2} \quad (10)$$

so that v_e is now 0.22 cm/sec for $\Delta a = 1$ cm. For the shorter TE values, such as TE = 20 msec, equation 9 implies that v_e is now nine times bigger if Δt remains fixed. Usually Δt is reduced to 30 μsec so that $v_e = 0.33$ cm/sec. Obviously, small velocity changes can lead to significant ghosting even if there is no motion between views.

Abdominal motion is not limited to the subcutaneous fat but is significant for the liver, kidney, and other abdominal organs [12] as well as for the heart and associated vasculature. It is now not surprising that standard sequences with TE greater than 30 msec have not led to high-quality body images. In fact, ghosting, as well as spin dephasing across a pixel [15], also leads to a loss of signal for the main (central) image of the moving object [7, 16] since the periodic ghosts effectively steal energy from it. This can lead to low measured values of T2, a T2″ say, which could in turn lead to a misdiagnosis. For example, a single T2-weighted image of the liver could lead to the diagnosis of hemachromatosis [17] unless a rephasing sequence is used. The usual signal from in-plane blood flow is normally small because of spin dephasing. By using the rephasing sequences discussed in the following paragraphs, it should be possible to measure both T1 and T2 for blood.

One step toward removing the phase dependence on velocity at the echo is to rephase the spins with another gradient [18]. Introducing this extra gradient allows both the stationary and constant-velocity moving spins to be refocused simultaneously [19–23]. Using two extra gradients allows even constant accelerating spins to be refocused [23]. It is the purpose of this paper to show the tremendous clinical utility of these new refocused sequences. To this end, we will consider first the phase behavior for the latter case of two extra gradients or a bipolar-gradient refocusing scheme, even though a single extra gradient would suffice.

The idea of phase encoding flowing spins by using extra gradients is not new [24, 25]. Rather than using the phase information to velocity-encode the blood flow, introducing these bipolar gradients as in Figure 1B, which act as an even echo-rephasing mechanism, can set the phase at the echo to zero for any spin moving with constant velocity. In this case, the phase as a function of time is

$$\phi(x,t) = \gamma G_1 xt + \gamma G_1 vt(2\tau + \tfrac{1}{2}t)$$
$$+ \gamma v[G_1(t_2 - t_1)(2\tau - \tau_2) + G_2(t_3 - t_2)(t_2 + t_3 - t_1 - 2\tau)] \quad (11)$$

The time-independent, but velocity-dependent phase term (in square brackets) can be made to vanish independently of the velocity. The flexibility alluded to above is evident in the phase term. Of the five variables G_1, G_2, t_1, t_2, and t_3, only three are independent since there are two constraints on the system. They are (1) the zero moment with respect to time must be γGxt and (2) the first moment must be zero at the echo. We shall discuss later how these choices are made.

Carefully calibrating the gradients and timing to obtain zero phase at the echo is crucial in a practical implementation of this sequence. Even small calibration errors can lead to significant phase effects when the velocities are large. Further difficulties arise because of finite gradient rise times and eddy currents. The form of the time-dependent terms remains unchanged by the additional rephasing gradients. For blood-flow imaging, cardiac gating would help remove most remaining phase changes between views to avoid periodic artifacts.

The gradient G_2 must be chosen as a function of G_1 from equation 11 so that the phase term vanishes. This condition gives

$$G_2 = G_1 \frac{(2\tau - t_2)(t_2 - t_1)}{(2\tau + t_1 - t_2 - t_3)(t_3 - t_2)} \quad (12)$$

$$= G_1 \frac{(2\tau - t_2)}{(2\tau - 3t_2)} \quad (13)$$

for $t_1 = 0$ and equal length gradients G_1 and G_2 before the π pulse ($t_2 - t_1 = t_3 - t_2$). For long TE values (TE = 2τ) and short sampling times, the value of G_2 is close to that of G_1. Values of t_1, t_2, and t_3 can be chosen to minimize G_2 or keep gradient times short if eddy currents are a problem. The optimal value of G_2 will be G_1 so that no loss of potential resolution is incurred. This is important for systems with only low-gradient capabilities or if high-resolution (small-field-of-view) imaging is desired [19]. The value of G_1 is set by the usual imaging constraints on field of view and Nyquist frequency, while t_1 and t_3 are chosen to minimize phase effects due to accelerating spins.

These sequences can be used for high signal-to-noise flow measurements. By dephasing the sequences slightly so that only a small loss of signal occurs, but enough to give the phase a sufficiently strong velocity-dependent term, flow measurements via the phase are possible. Likewise, spin-dephasing effects can be used to advantage by dephasing the spins to eliminate signal from fast laminar flow as in the femoral or carotid artery but not in the veins. This allows for arterial and venous identification by subtracting the dephased images from the rephased images [19].

Materials and Methods

Standard spin-echo sequences (as in Fig. 1A) from a Siemens 1.0-T and 1.5-T Magnetom were used as the starting point. These sequences were modified as shown in Figure 1B and calibrated so that the phase of moving spins was identical to that of stationary spins. This was accomplished by using plexiglass tubes, one of which had stationary spins, one of which had laminar flow with a mean velocity of +10 cm/sec, and one of which had a velocity of −10 cm/sec. In the phase reconstruction of the images, the tubes could not be distinguished after calibration. Whereas, if the calibration was imperfect, phase profiles varied across the diameter of the tubes and were indicative of the relative direction of flow and could be quantitatively related to velocity.

The two main sequences used were a TE = 38 msec and a TE = 60 msec sequence. The sampling intervals were 30 μsec and 70

μsec, respectively, with the number of sampling and phase-encoding points both being 256 unless otherwise stated. With t_2 = 8 msec, this leads to values of $G_2 = 2.1G_1$ in the first case and $G_2 = 1.44G_1$ for the second case. To allow for the optimal system, small-field-of-view capabilities (i.e., keeping $G_1 = G_2$) and shorter echoes, only three gradients (Fig. 1C), were used in the TE = 38 msec sequence (so that only constant-velocity terms are eliminated). Even so, by adjusting the position and amplitudes of the gradients, the effects of acceleration were also minimized. A TE of 38 msec also allows for rephasing in the slice-select direction.

Results

In order to illustrate the difference in image quality between standard (dephased) and rephased spin-echo sequences, images are presented for both scans. Figure 2 shows a sagittal spine image with a long TE value of 60 msec. Motion degradation significantly reduces signal-to-noise ratio and contrast between the spine and spinal cord (Fig. 2A). The rephased image (Fig. 2B) shows an image that is much more useful diagnostically with large signal from the CSF. No motion artifacts remain. This allows for improved CSF contrast with TR values shorter than 2 sec.

Body scans are often deemed useless because of the ghosting artifacts caused by respiratory motion. In fact, for long TE values, significant blurring or loss of signal may occur. An example of decreased liver signal and blurring is shown in Figure 3. The first scan has very poor resolution and signal-to-noise ratio. The rephased image shows the lack of ghosting or jitter throughout the liver and hence the apparent improvement in resolution. Neither scan was respiratory gated. Even so, the rephased image shows much sharper boundaries and much less blurring than its normal counterpart. A second example is shown in Figure 4 for a sagittal cut. The maximum signal from the liver in the rephased image is 650 units with a background noise of 30 units. The remaining respiratory artifacts are coherent edges with 70 units maximum amplitude. In the dephased image, the ghosts are 130 units and spread throughout the body. Most of the energy from these ghosts has been returned to the central image by rephasing. A background noise of 50 units in the region of the moving

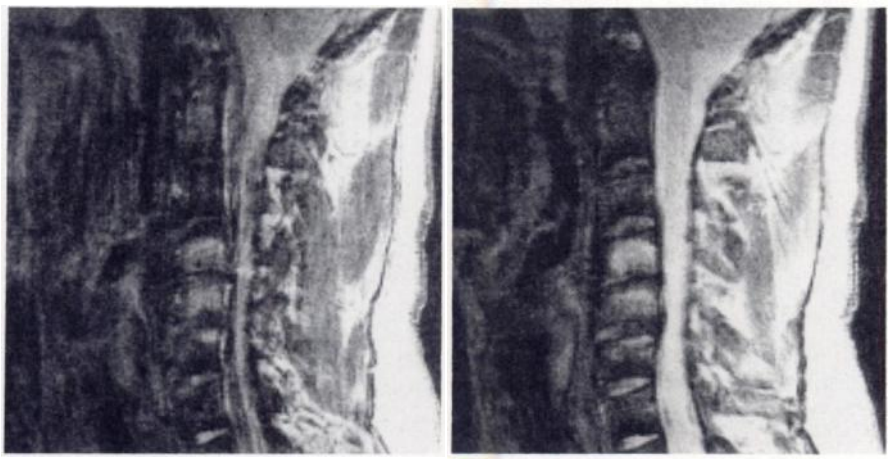

Fig. 2.—A comparison between a standard (*A*) and rephased (*B*) sequence with TR = 2 sec and TE = 60 msec; a surface coil was used. Slice thickness is 4 mm. Contrast between spine and CSF is greatly enhanced in *B* because of reduction of motion artifacts and increased signal from CSF.

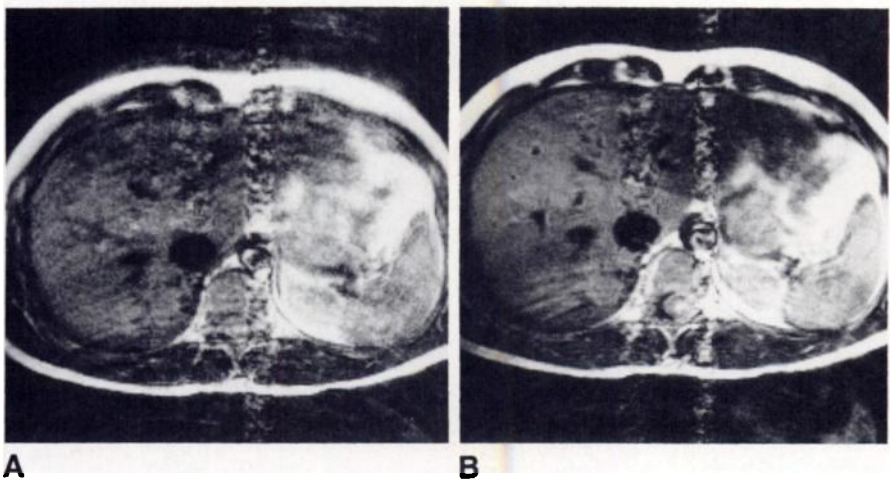

Fig. 3.—Ungated T1-weighted comparison between a standard (*A*) and rephased (*B*) sequence with TR = 400 msec, TE = 60 msec, four acquisitions, and 10-mm slice thickness. Standard image is smeared, especially the liver. Rephased image displays a coherent liver and much improved boundary enhancement. Neither image is respiratory gated.

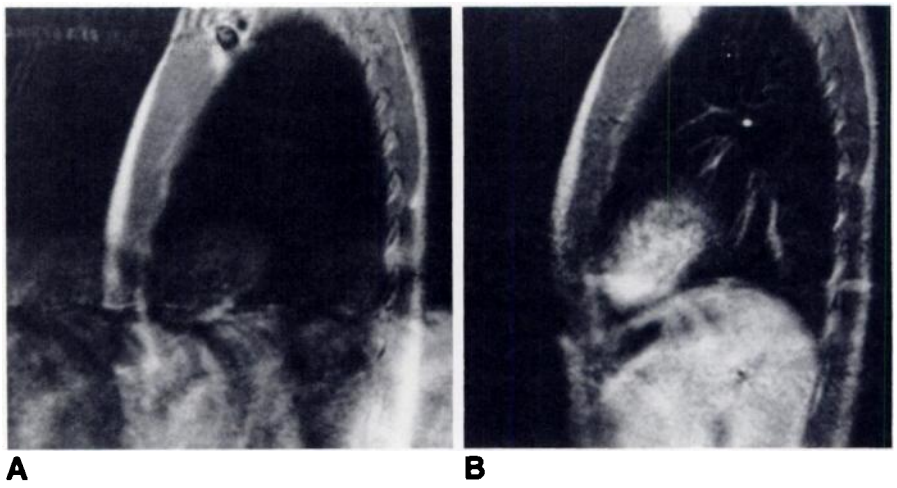

Fig. 4.—Same as Fig. 3, but with TR = 500 msec, TE = 38 msec, and 20-mm-slice thickness. Note blurring and loss of signal through liver and edge of heart in normal image (*A*). Most signal from liver, heart, and some flowing blood in the pulmonary arteries has been recovered in rephased image (*B*).

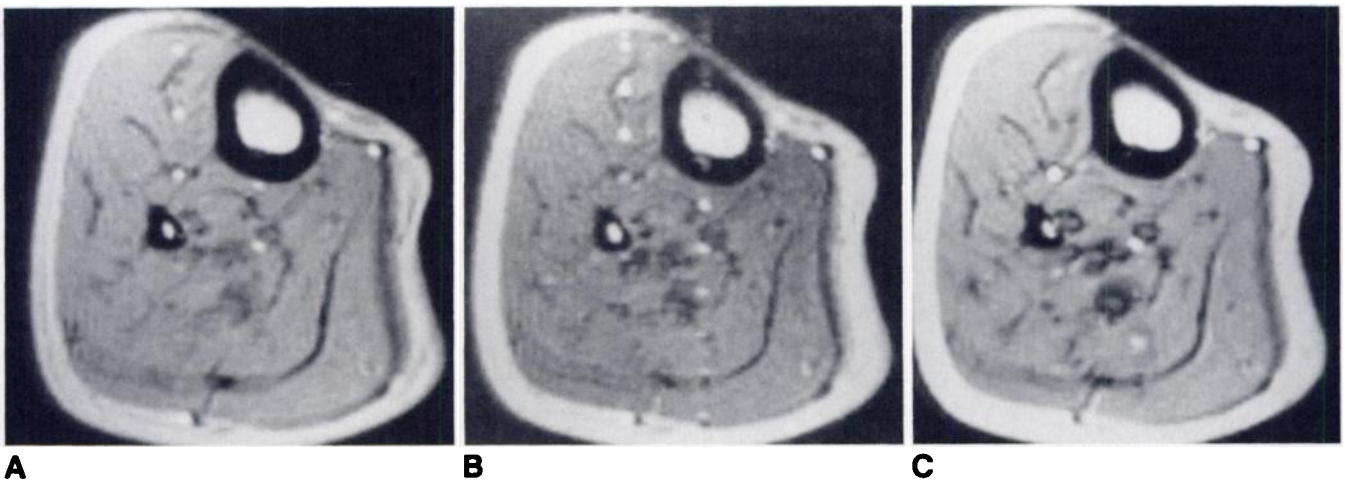

Fig. 5.—Effect of random phase variations due to motion in slice-select direction is expected to be reduced by reducing TE. Even this is not enough for fast flow, as is shown in gradient-echo sequence of *A* with TE = 10 msec, TR = 50 msec, a sampling rate of 30 μsec, and a slice thickness of 10 mm. Increasing TE to 20 msec (*B*) shows an increase in ghosting from pulsatile blood flow. Rephasing in slice-select direction significantly reduces artifacts (*C*) even with TE still at 20 msec.

organs still remains, perhaps because of unrefocused signal in the other two directions. The reduction in artifacts comes from the elimination of the random-phase term proportional to *v* and is exceptional considering that there is no respiratory gating. Also, signal in the blood in the pulmonary arteries has increased. These remarks are valid for fast gradient-echo sequences too.

Fast, low-angle shot (FLASH) imaging can also be expected to show the blood [11] because of the short TE values used; but when the image is ungated, as in volume imaging, the heart or other body parts will not have sharp boundary definition [5]. However, even short TE values of 10 msec may be insufficient to eliminate ghosting (Fig. 5A). The pulsatile nature of blood flow through the plane is enough, even for plug flow, to cause a periodic phase change in the signal. By using TE = 20 msec, the effect is even worse. Nevertheless, the ghosting has been nearly eliminated for the TE = 20 msec sequence when the spins are refocused in the slice-select direction (Fig. 5C). The other vessels in the center of the muscle are now more clearly outlined as the phase blurring has been reduced.

A similar comparison study can be done in the heart to see the different components of flow. Figures 6A, 6B, and 6C show cardiac-gated images with no rephasing, with rephasing in the read direction, and with rephasing also along the slice-select direction respectively. Figure 6A is badly dephased with little signal from the myocardium. Figure 6B shows the muscle wall clearly with the remaining black regions due to flow perpendicular to the plane. Figure 6C clearly displays the fresh blood flowing into the plane (paradoxically enhanced). General vessel enhancement also appears in the diaphragm region. The potential of studying blood flow and heart-wall motion is now evident. Without rephasing, nonuniform motion may cause a loss of signal on the edges of valves or other

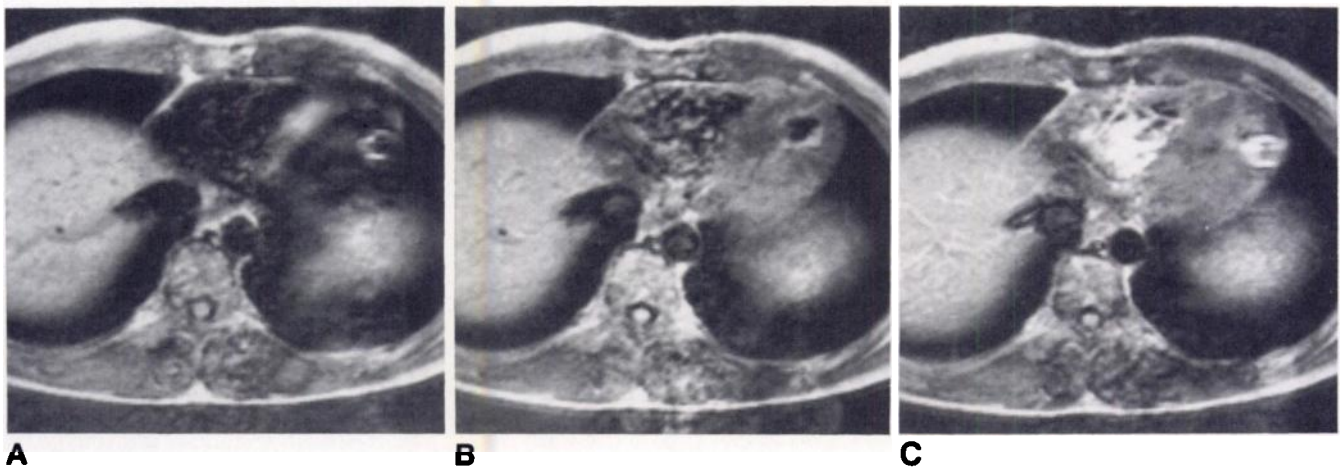

Fig. 6.—Cardiac-gated comparisons between a normal spin-echo sequence (*A*), a rephased sequence in the read (horizontal) direction (*B*), and a rephased sequence in both the read and slice-selection directions (*C*). All scans have a TE of 38 msec and a slice thickness of 10 mm. Signal from in-plane blood flow is enhanced in *B*, while a comparison between *B* and *C* illustrates flow perpendicular to the plane.

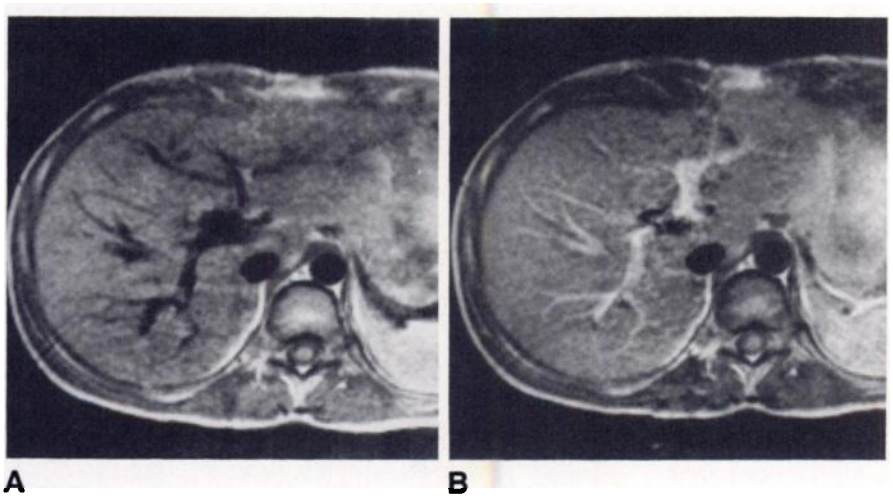

Fig. 7.—Portal vein and its branches are absent in liver in dephased sequence (*A*), but are bright in rephased sequence (*B*). Although vessels are visible in that they are black in dephased image, there is no ambiguity as to what is vessel and what might otherwise have been black in rephased image. TE = 38 msec and slice thickness is 10 mm.

moving cardiac muscle, which could be misinterpreted as a defect. Estimating T2 in the heart to correlate with ischemia, for example, will be extremely suspect unless the rephasing sequence is use.

The cardiac-gated image showing branching of the pulmonary artery in the lungs (Fig. 4B) shows the application of these principles to vascular imaging. The bright circle of blood in the center of the lungs is due to the rephasing in the slice-select direction and paradoxical enhancement, and it may occur at the confluence of several vessels. Blood flow in the liver and pancreas (Fig. 7) is also now easily discerned. Potential applications to renal arteries and other problems are numerous. In-plane flow in vessels such as the femoral artery can be seen by subtracting dephased from rephased images. The MR angiograms compare well with the accompanying digital subtraction angiogram (Fig. 8). A crucial point is that the use of equal-amplitude gradients ($G_1 = G_2$) in the read direction also allows small fields of view [19].

Discussion

Body imaging without gating usually is of poor quality; this has been blamed on periodic motion artifacts generated by motion between phase-encoding views [8, 9]. The fact that velocity may vary from zero to v between views leads to a phase variation from zero to the maximum value given in equation 4. For the TE = 60 msec sequence defined earlier, this gives a maximum phase deviation of $1.07v$ radians with v in cm/sec. These large phase variations are the major source of ghosting as is evidenced by the significant reduction of artifacts upon rephasing. Since the velocity in the CSF is as high as 5 cm/sec, a phase variation of 5.35 radians for TE = 60 msec occurs and hence significant ghosting is expected (see Fig. 2A). For nonuniform or laminar flow, such large phase variations (almost 2π) can lead to a significant loss of signal via spin dephasing [15]. Both effects are seen in the spine.

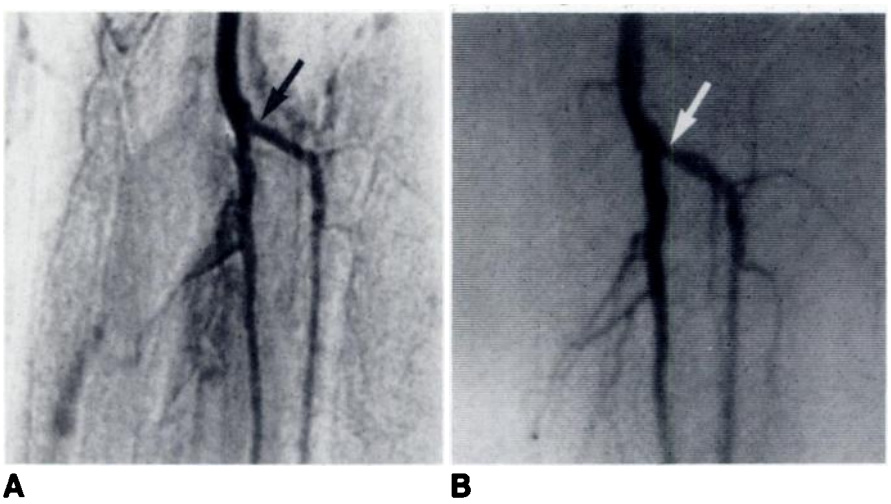

Fig. 8.—MR angiogram (*A*) obtained by subtracting a dephased image from a rephased image for cardiac-gated images with TE = 60 msec and a slice thickness of 10 mm. An angiogram (*B*) was taken several weeks before MR scans. Occlusion in anterior tibial artery was treated with urokinase.

Occlusion (*arrow*) is readily seen in angiogram whereas lumen of vessel near bifurcation now appears larger in the MR image.

In body imaging, when only rephasing gradients are used (Fig. 4B), the remaining artifact is a coherent ghost due to the familiar respiratory problem. Evidently, motion even perpendicular to the anteroposterior respiratory motion still causes severe artifacts. Both Figures 3 and 4 have the refocusing in the horizontal direction (perpendicular to the anteroposterior motion). Refocusing in all three directions independently is likely to further improve the image quality.

It is claimed that fast imaging techniques produce good quality images (as long as breath-holding is possible). One reason for the improvement in the quality of scans is the short TE value employed, often as low as 10 msec. For TE = 10 msec, $G = 4\ mT/m$ and v in cm/sec, according to equation 6, the phase at the echo is $0.027v$ radians. As expected, the resulting images are almost artifact free for low velocities. For fast-flowing blood (v can be 100 cm/sec), this will not be true even for this short TE value since as v varies from view to view, significant phase variation occurs. Similar dephasing occurs for the usual slice-select gradients. Rephasing in the slice-select direction helps to reduce any pulsation artifacts, as illustrated in Figures 5A, 5B, and 5C.

The ability to rephase moving spins can actually be detrimental in cardiac imaging. Although fast cinemode imaging is attractive for some diagnostic studies, the increased signal from the blood can eliminate contrast with myocardium and lead to signficant motion artifact for imperfect cardiac gating or rephasing because the signal from the blood is now so bright. When rephasing gradients are used in the heart, even in both slice-select and read directions, all blood may not be refocused. For example, if only constant-velocity spins are refocused, then accelerating or turbulent spins can give ghosting or regions with no signal (because of spin dephasing). The refocusing in Figure 6B, although good, was incomplete, as shown in Figure 6C where rephasing was also applied in the slice-select direction. Great care should therefore be taken in interpreting such cardiac images.

The important practical aspect of these rephasing sequences is that the potential field of view can escape unscathed by adding an extra gradient to the sequence. This is particularly crucial to short-TE imaging or for high-resolution flow imaging. With rise times of 1.5 msec and RF pulse times of 2.5 msec, a rephased gradient-echo sequence can be constructed for TE = 17 msec while a spin-echo sequence of TE = 23 msec is possible. All gradient amplitudes are the same as the usual read gradient of 2.6 mT/m for a 30-cm field of view. For a 6-mT/m system, 0.5-mm resolution can be attained. By increasing the TE value and the sampling time, the read gradient can be reduced to allow for a smaller field of view. For example, cutting G in half doubles the potential resolution and increases the signal-to-noise ratio by $\sqrt{2}$.

Conclusions

Motion has long been the bane of MR body imaging because of respiration, peristalsis, and flow both between views and during gradient applications. The latter causes not only ghosting but also spin dephasing and the associated loss of signal, especially for T2-weighted images. Practical examples have illustrated the importance of eliminating the velocity-dependent phase variations by using rephasing sequences. Not only is ghosting significantly reduced, but the spin dephasing is essentially removed, returning the signal to that which would have been obtained had there been no movement at all. This was found most useful for (1) organs affected by respiratory motion such as the liver, pancreas, and kidney; (2) CSF; and (3) blood flow. The phase correction can be made in spin-echo and fast gradient-echo sequences, for long or short TE values, and with multiecho, multislice imaging. Combining rephasing with respiratory gating, ordered phase encoding, or some motion-correction scheme should help to make body imaging more widely used in MR imaging.

REFERENCES

1. Runge VM, Clanton JA, Partain CL, James AE. Respiratory gating in magnetic resonance imaging at 0.5 Tesla. *Radiology* **1984**;151:521–523

2. Bydder GM, Young IR. MR imaging: clinical use of the inversion recovery sequence. *J Comput Assist Tomogr* **1985**;9:659–675
3. Haase A, Frahm J, Haenicke W, Matthaei D. ^{1}H-NMR chemical shift selection (CHESS) imaging. *Phys Med Biol* **1985**;30:341–344
4. Haacke EM, Lenz GW, Nelson AD. Pseudo-gating: elimination of periodic motion artifacts in magnetic resonance imaging without gating. *Mag Resonance Med* **1987**;4:162–174
5. Stark DD, Ferrucci JT. Technical and clinical progress in MRI of the abdomen. *Diagn Imag Clin Med* **1985**;11:118–127
6. Bailes DR, Gilderdale DJ, Bydder GM, Collins AG, Firmin DN. Respiratory ordered phase encoding (ROPE): a method for reducing motion artifacts in MR imaging. *J Comput Assist Tomogr* **1985**;9:835–838
7. Haacke EM, Patrick JL. Reducing motion artifacts in two dimensional Fourier transform imaging. *Mag Resonance Imaging* **1986**;4:359
8. Haacke EM. Solving for non-ideal conditions in two-dimensional Fourier transform imaging. *Inverse Problems* (in press)
9. Cuppen JJM, Groen JP, In der Kleef JJE, Tuithof HA. Reduction of motion artifacts by data post processing. Presented at the annual Society of Magnetic Resonance in Medicine Conference, London, August **1985**: 962–963
10. Haacke EM, Bearden FH, Clayton JR, Linga NR. Reduction of MR imaging time by the HYBRID fast scan technique. *Radiology* **1986**;158:521–529
11. Frahm J, Haase A, Matthael D. Rapid NMR imaging of dynamic processes using the FLASH technique. *Mag Resonance Med* **1986**;3:321–327
12. Suramo I, Paivansalo M, Myilyla V. Cranio-caudal movements of the liver, pancreas, and kidneys in respiration. *Acta Radiol Diagn* **1984**;25:129–131
13. van Dijk P. Direct cardiac imaging of heart wall and blood flow velocity. *J Comput Assist Tomogr* **1984**;8:429–436
14. Barth K, Deimling M, Fritschy P, Lenz G, Mueller E, Reinhardt ER. Visualization and measurement of flow within magnetic resonance imaging. *Biomed Technik* **1985**;30:12–17
15. Wehrli F, MacFall JR, Axel L, Shutts D. MR imaging of venous and arterial flow by a selective saturation–recovery spin echo (SSRSE) method. *J Comput Assist Tomogr* **1985**;9:537–545
16. Wood ML, Henkelman RM. Image artifacts from periodic motion. *Med Phys* **1985**;12:143–151
17. Stark DD, Wittenberg J, Edelman RR, et al. Detection of hepatic metastasis by magnetic resonance: analysis of pulse sequence performance. *Radiology* **1986**;159:365–370
18. Nishimura DG, Macovski A, Pauly DM. Magnetic resonance angiography. *IEEE Trans Med Imag* **1986**;MI-5:140–151
19. Lenz GW, Haacke EM. High resolution, signal-to-noise flow quantification vascular imaging. Presented at the annual Society of Magnetic Resonance in Medicine Conference, Montreal, August **1986**:88–89
20. Constantinesco A, Mallet JJ, Bonmartin A, Lallot C. Spatial or flow velocity phase encoding gradients in NMR signals. *Mag Resonance Imaging* **1984**;2:335–440
21. Axel L, Morton D. A method for imaging blood vessels by phase compensated/uncompensated difference images. *Mag Resonance Imaging* **1986**;4:153
22. Naylor G, Firmin DN. Multislice MRI angiography. *Mag Resonance Imaging* **1986**;4:156
23. Pattany PM, Marion R, McNally JM. Velocity and acceleration desensitization in 2DFT, MR imaging. *Mag Resonance Imaging* **1986**;4:154–155
24. Moran PR. A flow velocity zeugmatographic interlace for NMR imaging in humans. *Mag Resonance Imaging* **1982**;1:197–203
25. Bryant DJ, Payne JA. Measurement of flow with NMR imaging using a gradient pulse and phase difference technique. *J Comp Assist Tomogr* **1984**;8:588–593